Atomistic modeling of grain boundary motion as a random walk

Dengke Chen and Yashashree Kulkarni*
Department of Mechanical Engineering, University of Houston, Houston, Texas, USA

(Received 7 February 2018; published 12 September 2018)

Mechanical behavior of polycrystalline materials, such as creep and microstructural evolution, is dramatically impacted by the mobility of grain boundaries. Existing methods for extracting mobility that combine atomistic simulations with conventional Brownian-like random walk model for grain boundary motion miss critical insights and are reliable only above very high (and unrealistic) temperatures. In this paper, we present a computational method based on the classical Green-Kubo relation for computing interface mobility over a wide range of temperatures. Our study makes an intriguing revelation that the severe time limitation of molecular dynamics simulations warrants the use of a generalized diffusion equation for Brownian particles not accounted for in current studies. Moreover, the method furnishes analytical expressions for the interface mobility in terms of the velocity autocorrelation functions. Taken together, our results possibly provide the first reliable estimates for interface mobility in the limit of zero driving forces. This is in sharp contrast to studies based on the widely used interface random walk approach, which extracts mobility by fitting the conventional Brownian motion equation to atomistic simulations. The efficiency of the method and applicability over a range of temperatures should open avenues for integration of computations and experiments to understand and engineer material systems with desired properties.

DOI: 10.1103/PhysRevMaterials.2.093605

I. INTRODUCTION

Grain boundary (GB) mediated processes such as sliding, migration, and interaction with other defects, play a vital role in plasticity, damage, and failure in polycrystalline materials, including structural metallic systems, and have been the subject of longstanding interest [1–16]. The kinetics of these crystalline interfaces is governed by a key parameter, the grain boundary mobility, which is an intrinsic property of the grain boundary that dictates grain boundary migration, and hence, the microstructural evolution and the concomitant evolution of material properties. Taking into account the structural dependence and environmental factors, the interface mobility M, is the coefficient relating the exerted pressure F and the migration or normal velocity of the grain boundary v through the well-known relation, $v = MF$.

With rapid advances in high-performance computing, atomistic methods, such as molecular dynamics (MD), are being increasingly used to investigate grain boundary mobility [17–29], especially since controlled experiments are challenging to perform. Based on the thermal fluctuations of interfaces, Trautt *et al.* [23] introduced a novel computational method, the so-called interface random walk method, to capture the interface mobility in the zero driving force limit. The approach is based on monitoring the mean interface displacement along the direction normal to the (flat) interface at high temperatures, typically about 0.8 homologous temperature. By regarding this motion as a random walk, the fluctuation-dissipation relation is invoked to furnish the interface diffusion equation $\langle \bar{h}^2 \rangle = Dt$ in terms of the variance of the mean boundary displacement, $\bar{h}(t)$ (see Fig. 1). The diffusion coefficient associated with this Brownian motion is then related to the interface mobility as $D = \frac{2Mk_BT}{A}$, where A is the area of the interface. Deng and Schuh [25,26] proposed an interesting postprocessing approach, and showed that it extended the application of the interface random walk approach to low temperatures, up to 0.2 homologous temperature. In recent years, the interface random walk model has been widely used for predicting the absolute interface mobilities in various materials systems.

In this paper, we seek to ascertain the theoretical basis of the random walk model for grain boundary motion and explore its limitations, if any, over a range of temperatures. Our study furnishes a rather unexpected but critical insight into a shortcoming of conventional approaches that combine atomistic simulations with the random walk model for grain boundary motion and how it can be circumvented. Specifically, we show that, owing to the severe time limitation of molecular dynamics simulations, it is imperative to use a generalized diffusion equation for the Brownian motion in order to correctly represent grain boundary migration as a random walk. This is in contrast to existing studies based on the interface random walk method, which use the conventional diffusion equation for the interface mentioned before. This intriguing insight sets the stage for an alternative efficient computational scheme based on the classical Green-Kubo relations [30,31] for computing grain boundary mobility in the limit of zero driving forces. A further advantage over the interface random walk approach is that this method yields analytical expressions for the mobility in terms of the velocity autocorrelation functions.

*ykulkarni@uh.edu

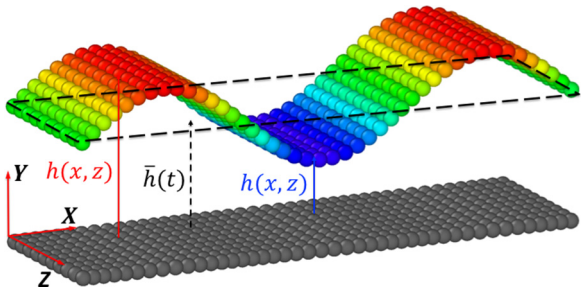

FIG. 1. Schematic of a fluctuating grain boundary exhibiting normal motion. The gray atoms represent the initial mean position of the grain boundary taken as the reference. The instantaneous interface height profile is denoted by $h(x,z)$. The dashed black line marks the instantaneous mean position of the grain boundary with the mean boundary displacement denoted by $\bar{h}(t)$.

II. THEORY

A. Generalized boundary diffusion equation

We begin by deriving the generalized diffusion equation for a grain boundary regarded as a Brownian particle in terms of its mean-square displacement. To this end, let us first introduce the mean boundary displacement, $\bar{h}(t)$, defined as the average displacement of every atom residing in the grain boundary in the direction of migration at time t (see Fig. 1). We then define a new variable, $s(i)$, as the incremental mean boundary displacement from time $t_{i-1} = (i-1)\Delta t$ to $t_i = i\Delta t$ such that $s_j(i) = \bar{h}_j(i) - \bar{h}_j(i-1)$. Here, $j = 1, 2, \ldots, N$ denotes number of simulation samples, and $i = 2, \ldots, n$ denotes the number of time intervals of sampling. We assume $s_j(1) = \bar{h}_j(1)$.

Introducing $\bar{v}(i) = s(i)/\Delta t$ as the average grain boundary velocity in the time interval from t_{i-1} to t_i, the velocity autocorrelation function for the grain boundary motion can be expressed as [32]

$$R(k) = \langle \bar{v}_j(i)\bar{v}_j(i+k)\rangle = \frac{1}{\Delta t^2}\frac{1}{n-k}\sum_{i=1}^{n-k}\left[\frac{1}{N}\sum_{j=1}^{N} s_j(i)s_j(i+k)\right]. \quad (1)$$

We further note that the boundary displacement is the accumulated incremental displacement, that is, $\bar{h}_j(t) = \sum_{i=1}^{n} s_j(i)$. Then, the mean-square displacement can be evaluated in terms of the velocity autocorrelation functions using Eq. (1). It is rather surprising that $\langle \bar{h}^2(t)\rangle$ obtained from velocity autocorrelations has the form

$$\langle \bar{h}^2(t)\rangle = Dt + C, \quad (2)$$

which we refer to as the generalized interface diffusion equation. Here, $C = -2(\Delta t)^2 \sum_{k=1}^{n-1} kR(k)$ and $t = n\Delta t$. The grain boundary diffusion coefficient D is obtained as

$$D = \Delta t\left[R(0) + 2\sum_{k=1}^{n-1} R(k)\right]. \quad (3)$$

The ramifications of this derivation are many. First, we remark that the derivation presented here is based on the Langevin theory of Brownian motion according to which the mean-square displacement of a Brownian particle contains a constant term and an exponentially decaying term, in addition to the term linear in time [33]. However, at t sufficiently large, these terms are neglected to yield the well-known diffusion equation for a random walk, $\langle \bar{h}^2\rangle = Dt$. While working on long time scales, typically in theoretical analyses and simulations of macroscopic systems, this assumption works well. However, when using MD simulations to study Brownian motion, which provides data spanning a few hundred picoseconds at best, this assumption requires scrutiny. Indeed, as is illustrated by our MD simulations, the effect of the intercept C in Eq. (2) cannot be ignored, except at high temperatures. In other words, it is the severe time limitation of atomistic simulations that warrants the use of the generalized diffusion equation for Brownian particles, which is not taken into account in current studies based on the interface random walk approach and which may lead to considerable errors in mobility estimates.

Second, Eq. (3) illustrates that the autocorrelation functions furnish an analytical expression for grain boundary diffusion coefficient, which is in contrast to the interface random walk approach, where D is extracted by fitting the conventional diffusion equation to atomistic simulations. We would like to note that Deng and Schuh [26] also obtained a similar equation as our Eq. (2) but they only considered the correlation between adjacent time intervals. Thus, their definitions for D and C were different (or rather incomplete) compared to the expressions derived in this work. Later, we will present our simulation results, which highlight the importance of considering the full autocorrelation function as opposed to just adjacent time intervals.

Finally, the derivation of the generalized boundary diffusion equation opens an avenue for computing grain boundary mobility based on the classical Green-Kubo relation, which expresses transport coefficients in terms of integrals of velocity autocorrelation functions. The details of the derivation are provided in the next section.

B. Green-Kubo relation for grain boundaries

We begin by considering a bicrystal containing a GB with periodic boundary conditions in lateral (X and Z) directions. At finite temperature, the height profile $h(\mathbf{r}, t)$ of the fluctuating GB is shown in Fig. 2. Following the classical GB migration relation from kinetic theory, we have

$$v(\mathbf{r}, t) = MF(\mathbf{r}, t), \quad (4)$$

where the coordinate $\mathbf{r} = (x, z)$ is restricted to the interfacial plane, and $F(\mathbf{r}, t)$ is the force acting on the GB. According to the Langevin theory of Brownian motion, the force $F(\mathbf{r}, t)$ includes thermal noise $\xi(\mathbf{r}, t)$ and a curvature restoring force $f_c(\mathbf{r}, t)$. The thermal noise is treated as a Langevin force associated with thermal fluctuations and is assumed to be uncorrelated [23]. That is,

$$\langle \xi(\mathbf{r}, t)\xi(\mathbf{r}', t')\rangle = \frac{2k_BT}{M}\delta(\mathbf{r} - \mathbf{r}')(t - t'). \quad (5)$$

Under the small slope approximation $h_x \ll 1, h_z \ll 1$, the curvature restoring force f_c is given by

$$f_c(\mathbf{r}, t) = \Gamma(h_{xx} + h_{zz}), \quad (6)$$

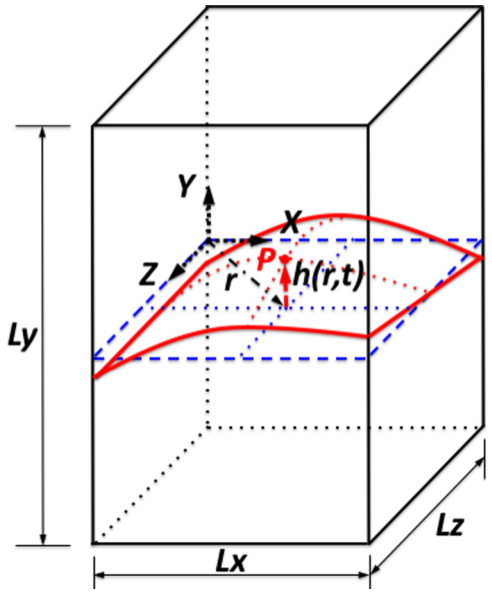

FIG. 2. Schematic showing the thermal fluctuations of a grain boundary. The blue dotted line represents the mean GB profile; red solid line corresponds to the actual fluctuating GB.

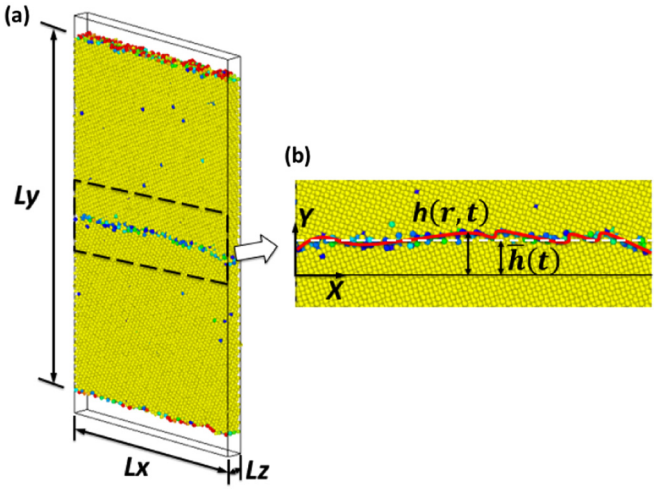

FIG. 3. (a) Atomistic configuration of the MD simulation cell with a Σ5(310)[001] GB visualized using OVITO [35]. (b) Snapshot of the fluctuating grain boundary at finite temperature with atoms colored using centrosymmetry parameter. The red curve indicates the instantaneous height profile, $h(\mathbf{r}, t)$, and the dashed white line marks the mean boundary displacement, $\bar{h}(t)$, of the fluctuating grain boundary.

where Γ is known as the GB stiffness [34] and h_{xx} and h_{zz} are the principal curvatures. Then Eq. (4) can be rewritten as

$$v(\mathbf{r}, t) = \frac{\partial h(\mathbf{r}, t)}{\partial t} = M[\Gamma(h_{xx} + h_{zz}) + \xi(\mathbf{r}, t)]. \quad (7)$$

We define the mean GB displacement, $\overline{h}(t)$, as the average displacement of every atom residing in the grain boundary in the direction of migration at time t. That is,

$$\overline{h}(t) = \frac{1}{A}\int_0^{L_x}\int_0^{L_z} h(\mathbf{r}, t)dxdz, \quad (8)$$

where $A = L_x L_z$ is the GB area. Similarly, the mean GB migration velocity $\overline{v}(t)$ can now be defined as

$$\overline{v}(t) = \overline{\frac{\partial h(\mathbf{r}, t)}{\partial t}} = \frac{1}{A}\int_0^{L_x}\int_0^{L_z} M[\Gamma(h_{xx} + h_{zz}) + \xi(\mathbf{r}, t)]dxdz. \quad (9)$$

Due to periodicity along the X and Z directions, the spatial integral of the curvature restoring force vanishes. That is,

$$\frac{1}{A}\int_0^{L_x}\int_0^{L_z} M[\Gamma(h_{xx} + h_{zz})]dxdz = 0. \quad (10)$$

This yields

$$\overline{v}(t) = M\overline{\xi}(\mathbf{r}, t), \quad (11)$$

where $\overline{\xi}(t) = \frac{1}{A}\int_0^{L_x}\int_0^{L_z}\xi(\mathbf{r}, t)dxdz$ denotes the spatial average of the thermal noise. The velocity autocorrelation functions can now be defined as

$$R(\tau) = \lim_{Q\to\infty}\frac{1}{Q}\int_{-Q/2}^{Q/2} < \overline{v}(t)\overline{v}(t+\tau) > dt. \quad (12)$$

Combining Eq. (5), Eq. (11), and Eq. (12) together, we obtain

$$R(\tau) = \frac{2Mk_BT}{A}\delta(\tau). \quad (13)$$

Integrating both sides and taking into account that $R(\tau)$ is an even function (by definition), we obtain the classical Green-Kubo relation for the GB diffusion coefficient

$$D = \frac{2Mk_BT}{A} = 2\int_0^{\infty} R(\tau)d\tau. \quad (14)$$

The corresponding mobility M is then expressed as

$$M = \frac{A}{k_BT}\int_0^{\infty} R(\tau)d\tau. \quad (15)$$

The discrete form for this equation used to extract the GB mobility from atomistic simulations in our study is given by

$$M = \frac{A\Delta t}{k_BT}\left[R(0)/2 + \sum_{k=1}^{n-1} R(k)\right]. \quad (16)$$

It can be seen that the expression for D in Eq. (3) is exactly the discrete form of Eq. (14). Thus, the Green-Kubo relation furnishes an efficient way to estimate grain boundary mobilities based on velocity autocorrelation functions, which can easily be computed from MD simulations.

III. SIMULATIONS

For validation, we present MD simulations to estimate the mobility of a Σ5(310)[001] symmetric tilt grain boundary in a Nickel bicrystal (see Fig. 3). The size of the simulation cell was 13.3 nm × 22.2 nm × 1.0 nm with periodic boundary conditions in X and Z directions. The system was free to relax in the Y direction, which is normal to the boundary.

Simulations were performed using LAMMPS [36] at temperatures ranging from 400–1200 K. The embedded-atom (EAM)

interatomic potential by Ackland *et al.* [37] was employed. Energy minimization of the simulation cell was performed by using the heating-and-quenching approach outlined by Deng and Schuh [26]. To be specific, each system was first equilibrated at 1300 K for 25 ps under the NPT ensemble, then gradually annealed to the desired temperature for 25 ps, and subsequently relaxed at the desired temperature for another 25 ps. After this relaxation process, the sample was equilibrated for 2 ns under the NVT ensemble using the Nose-Hoover thermostat. The atomistic configuration of the simulation cell was observed every 1 ps. Using the approach described in our previous work [16,38], we extract the instantaneous profile of the grain boundary using the centrosymmetry parameter and determine its mean displacement $\bar{h}(t)$. The mean-square displacement is calculated by performing multiple simulations, in parallel with different initial random velocities in LAMMPS. Specifically, we used 20 independent runs to calculate the ensemble averages, which is consistent with existing literature [23–26].

To understand the effect of cell size and geometry, we note that for the cell dimensions used in our work and other similar studies [23,25], the type of boundary conditions normal to the interface appears to have a negligible effect on the thermal fluctuations of the interface. Specifically, we found very good agreement between the mobility values obtained by us using free boundary conditions and those reported by Deng and Schuh [25] using fully periodic boundary conditions for the $\Sigma5(310)$ grain boundary in Ni using the same interatomic potential at the same temperature. Furthermore, in-plane periodic boundary conditions with a ribbonlike geometry of the grain boundary may possibly introduce numerical artifacts in the calculation of the interface mobility. In their original paper on the random walk model, Trautt *et al.* [23] investigated the effect of doubling the in-plane dimensions as well as the effect of a square cross section (instead of a ribbon-shaped cross section). They reported that although the fluctuations in the interfacial height profile decreased, the slope of the variance, $\langle \bar{h}^2 \rangle$, versus time, which is used in the mobility calculations remained the same. Hence, similar ribbonlike geometries with periodic boundary conditions have been used in majority of the mobility studies in the literature [23,25]. We also performed additional simulations on our $\Sigma5(310)$ grain boundary with a square cross section for Cu and Ni at high temperatures. We found that the mobility values varied only negligibly with the cell size and shape.

To verify the effect of the number of samples on our mobility results, we also repeated our calculations for the Ni $\Sigma5(310)$ grain boundary using the Ackland *et al.* potential [37] based on 30 samples at two temperatures, specifically, 400 K and 1200 K. At 1200 K, the error was within 1%. At 400 K, the error was within 10%, which we believe is reasonable given that the absolute mobilities are on the order of 10^{-10}. Thus, at both low and high temperatures, we found a negligible effect of the number of samples beyond 20 independent runs. Figure 4 shows the velocity autocorrelation plots for the two cases (comparing results for $N = 20$ and $N = 30$), which show no discernible difference even up to 500 ps.

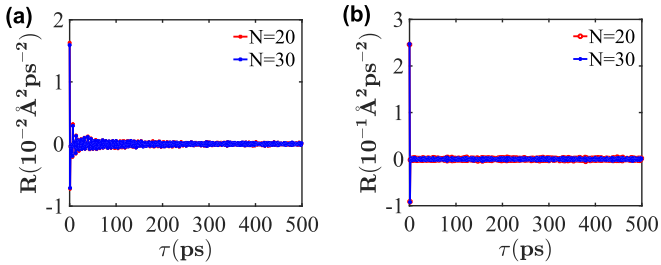

FIG. 4. The velocity autocorrelation function as a function of time at (a) 400 K, and (b) 1200 K, for $\Sigma5$ GB in Ni based on the potential developed by Ackland *et al.* [37] using 20 and 30 independent runs for obtaining the ensemble averages. The results show that there is negligible effect of the number of samples beyond 20 simulations.

IV. RESULTS AND DISCUSSION

Figures 5(a)–5(c) show the time evolution of the variance of mean grain boundary displacement $\langle \bar{h}^2(t) \rangle$ at 400 K, 800 K, and 1200 K, respectively. These temperatures cover a range from 0.2–0.7 homologous temperatures. Solid blue lines represent the linear regression curves based on fitting Eq. (2). We note that there indeed exists a finite intercept [see Figs. 5(a), 5(b)]. which needs to be accounted for in the calculation of the diffusion coefficient. At higher temperatures, as $\langle \bar{h}^2(t) \rangle$ grows orders of magnitude larger while the order of the intercept C does not change much, its effect becomes less important [see Fig. 5(c)]. In order to examine the intercept quantitatively, we performed curve fitting according to Eq. (2) and equation $\langle \bar{h}^2(t) \rangle = D_o t$ (without the intercept). The results for the latter are denoted by solid black lines in Figs. 5(a)–5(c). We introduce a parameter β defined as the ratio $\beta = D_o/D$. As temperature increases, β decreases and approaches unity denoted by the dashed black line in Fig. 5(d). This confirms that the effect of the intercept can be ignored at high temperatures, leading to the validity of the conventional interface random walk model. However, the intercept is significant at low temperatures, which are in fact physically

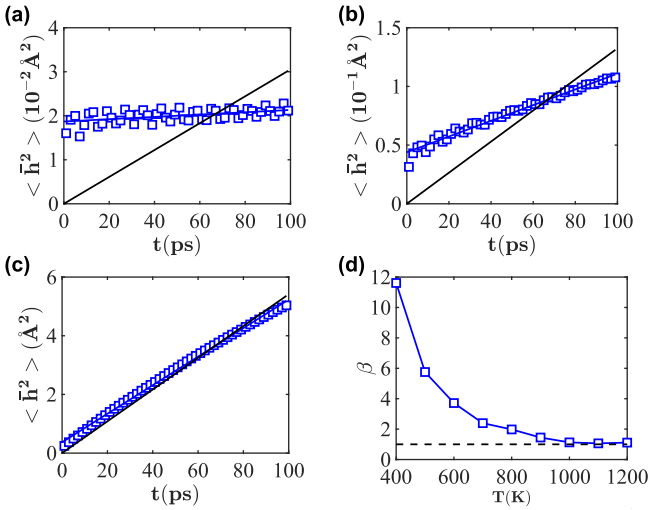

FIG. 5. Variance of mean grain boundary displacement for the $\Sigma5(310)[001]$ GB in Ni using the Ackland *et al.* potential [37] at (a) 400 K (b) 800 K, and (c) 1200 K respectively as a function of time obtained from MD simulations. (d) The temperature dependence of β over a range of temperatures.

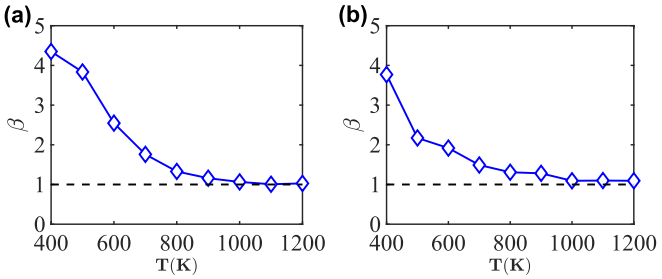

FIG. 6. The temperature dependence of the ratio β for (a) $\Sigma 5$ GB modeled using the Baskes *et al.* potential for Ni [39], and (b) $\Sigma 17$ GB modeled using the Mishin *et al.* potential for Cu [40].

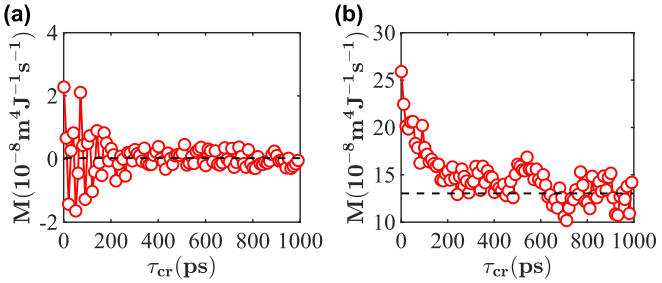

FIG. 8. Absolute grain boundary mobility calculated based on the Green-Kubo relation for the $\Sigma 5(310)[001]$ GB in Ni using the Ackland *et al.* potential at (a) 400 K, (b) 1200 K.

more relevant, and hence it should be incorporated in the computations of grain boundary mobility. To demonstrate this, we consider the temperature of 400 K where β is about 12. This indicates that if the interface random walk approach is applied, the mobility estimation should be off by an order of magnitude. We note that β also depends on the simulation time. At low temperatures, β would approach 1 and become independent of time only at much longer times (around few hundred nanoseconds and larger), which are beyond the scope of MD. Thus, its dependence on time again demonstrates the importance of considering the intercept at simulation times accessible to MD.

For further validation, simulations were also performed on the same $\Sigma 5(310)[001]$ grain boundary with a different Ni potential developed by Baskes *et al.* [39] (denoted as Σ5-Ni-Baskes) and on a $\Sigma 17$ (410) symmetric tilt grain boundary with a Cu potential developed by Mishin *et al.* (denoted as Σ17-Cu-Mishin) [40]. The results for the β parameter as a function of the temperature are presented in Fig. 6, which again support our conclusions and the proposed method.

Figures 7(a) and 7(b) show the velocity autocorrelation functions calculated at 400 K and 1200 K, respectively, based on Eq. (1) and plotted against time interval $\tau = k\,\Delta t$ where $k = 0, 1, 2, \ldots, n$ and $\Delta t = 1$ ps. Thus, $k = 1$ would yield the autocorrelation function considering only adjacent time intervals. It can be seen that the velocity autocorrelation functions, at both temperatures, are such that only the first two values (that is, for $k = 0$ and $k = 1$) are much more significant than the rest. This makes one wonder whether it suffices to consider only the adjacent time intervals like in the study by Deng and Schuh [26]. On the contrary, we demonstrate that the effect of the long tail cannot be ignored in the computation

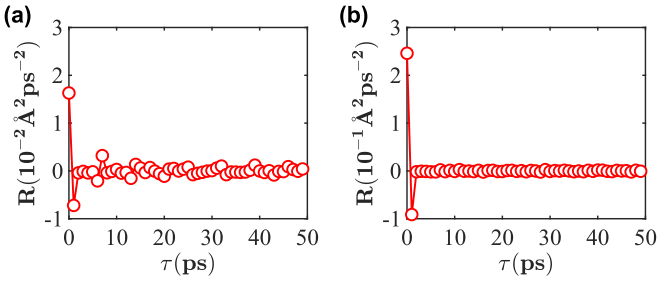

FIG. 7. Velocity autocorrelation function, $R(\tau)$, for the $\Sigma 5$ GB in Ni using the Ackland *et al.* potential at (a) 400 K, (b) 1200 K.

of the grain boundary mobility, especially at not very high temperatures.

To obtain the grain boundary mobilities according to Eqs. (15) or (16), we have to truncate the integral at some finite value of τ, which we refer to as $\tau_{cr}(= k_{cr}\Delta t)$ for the purpose of numerical calculations. Figures 8(a) and 8(b) show the plot for mobility versus $\tau_{cr}(\geqslant \Delta t = 1$ ps), at 400 K and 1200 K, respectively. It can be seen that after the initial dramatic fluctuations, the mobility converges to an asymptotic value, which we denote by M_{asym} (denoted by the black lines). In our calculations, we compute M_{asym} simply by taking an average over the mobility values in the time interval from 500–1000 ps. Specifically, at 400 K, the first data point represents $M = 2.28 \times 10^{-8}$ m^2 J^{-1} s^{-1} when $\tau_{cr} = 1$ ps, which is two orders of magnitude larger than the asympotic value, $M_{asym} = 2.71 \times 10^{-10}$ m^2 J^{-1} s^{-1} [Fig. 8(a)]. At 1200 K, $M = 2.59 \times 10^{-7}$ m^2 J^{-1} s^{-1} at $\tau_{cr} = 1$ ps, which is two times larger than the asymptotic value, $M_{asym} = 1.30 \times 10^{-9}$ m^2 J^{-1} s^{-1} [Fig. 8(b)]. In the two cases spanning a wide range of temperatures, mobility calculated by considering only adjacent time intervals for the autocorrelations is much larger than the asymptotic value and the difference diminishes only at high temperatures. This disparity is clear evidence that the long tail of the autocorrelation function cannot be neglected.

However, one question still remains: Which of these mobility values is the correct one? For this, we now compare the (asymptotic) mobility obtained from the Green-Kubo approach [Eq. (16)] with the mobility obtained by directly fitting the generalized diffusion equation [Eq. (2)] to MD data. We note here that although Figs. 5(a)–5(c) show data up to 100 ps, we perform linear regression over 1000 ps to be consistent with our Green-Kubo simulations. Figure 9(a) shows the semilog plot for M versus $1/k_BT$. It can be seen that the two computational methods are in excellent agreement. There is also a good agreement for the activation energy with only a small discrepancy (0.99 eV [Eq. (16)] $<$ 1.01 eV [Eq. (2)]) at high temperature. In the low-temperature regime, the activation energies are exactly the same. We also note that, as expected, M_{asym} follows the Arrhenius relation (red solid line), $M \propto \exp(-\frac{Q_m}{k_BT})$, but with two distinct regimes having different activation energies Q_m. This transition in grain boundary mobility above a certain temperature has been reported in prior works and is attributed to structural transitions in the boundaries as they exhibit a more liquidlike behavior above the transition temperature [25,29,41,42]. We

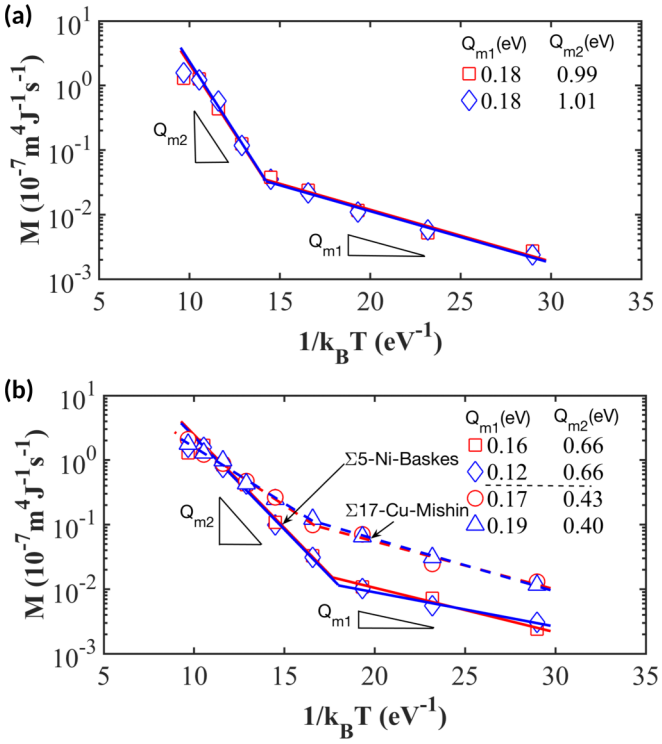

FIG. 9. Comparison of grain boundary mobility calculated using Green-Kubo formulation (marked in red) and the generalized interface diffusion equation (marked in blue) for (a) Σ5 boundary in Ni with the Ackland *et al.* potential [37]; (b) Σ5 boundary in Ni with the Baskes *et al.* potential [39] and Σ17 boundary in Cu with the Mishin *et al.* potential [40].

also performed a series of simulations on the same Σ5 grain boundary with another Ni potential [39] (denoted as Σ5-Ni-Baskes) and on a Σ17 symmetric tilt grain boundary with a Cu potential [40] (denoted as Σ17-Cu-Mishin). Figure 9(b) shows associated results, which also confirms the validity of the Green-Kubo method.

V. CONCLUSION

In summary, we present an efficient computational approach for calculating the mobility of grain boundaries by way of atomistic simulations in the limit of zero driving forces. The approach is based on the classical Green-Kubo relation and furnishes analytical expression for the boundary mobility in terms of the velocity autocorrelation functions. This makes the Green-Kubo approach naturally amenable over a wide temperature range. Finally, our study brings to light an important shortcoming of conventional atomistic simulations in modeling grain boundary motion as a random walk. It is revealed that there is a constant intercept in the generalized interface diffusion equation for Brownian motion, which is important to consider in estimating the grain boundary mobility owing to the time limitation of MD simulations. Taken together, our results possibly provide the first reliable estimates for interface mobility in the limit of zero driving forces over a wide range of temperatures. The efficiency and applicability of the method should open avenues for integration of computations and experiments to understand and engineer material systems with desired properties.

ACKNOWLEDGMENTS

We gratefully acknowledge the support of National Science Foundation under Grant No. DMR-1508484. The authors also acknowledge the use of the Maxwell Cluster and the support from the Center of Advanced Computing and Data Systems at the University of Houston.

[1] A. P. Sutton and R. W. Balluffi, *Interfaces in Crystalline Materials* (Oxford University Press, Oxford, 2007).
[2] G. Gottstein and L. S. Shvindlerman, *Grain Boundary Migration in Metals: Thermodynamics, Kinetics, Applications* (CRC Press, Boca Raton, 1999).
[3] E. O. Hall, The deformation and aging of mild steel: III discussion of results, Proc. Phy. Soc. Sect. A **64**, 747 (1951).
[4] N. J. Petch, The cleavage strength of polycrystals, J. Iron Steel Inst. **174**, 25 (1953).
[5] C. C. Koch, Optimization of strength and ductility in nanocrystalline and ultrafine grained metals, Scr. Mater. **49**, 657 (2003).
[6] C. A. Schuh, M. Kumar, and W. E. King, Analysis of grain boundary networks and their evolution during grain boundary engineering, Acta Mater. **51**, 687 (2003).
[7] T. Zhu and J. Li, Ultra-strength materials, Prog. Mater. Sci. **55**, 710 (2010).
[8] V. Agrawal and K. Dayal, A dynamic phase-field model for structural transformations and twinning: Regularized interfaces with transparent prescription of complex kinetics and nucleation. Part II: Two-dimensional characterization and boundary kinetics, J. Mech. Phys. Solids **85**, 291 (2015).
[9] C. Reina, L. Sandoval, and J. Marian, Mesoscale computational study of the nanocrystallization of amorphous Ge via a self-consistent atomistic phase-field model, Acta Mater. **77**, 335 (2014).
[10] A. T. Lim, M. Haataja, W. Cai, and D. J. Srolovitz, Stress-driven migration of simple low-angle mixed grain boundaries, Acta Mater. **60**, 1395 (2012).
[11] Y. Kulkarni and R. J. Asaro, Are some nanotwinned fcc metals optimal for strength, ductility and grain stability? Acta Mater. **57**, 4835 (2009).
[12] J. Bezares, S. Jiao, Y. Liu, D. Bufford, L. Lu, X. Zhang, Y. Kulkarni, and R. J. Asaro, Indentation of nanotwinned fcc metals: Implications for nanotwin stability, Acta Mater. **60**, 4623 (2012).
[13] X. W. Gu, Z. Wu, Y. W. Zhang, D. J. Srolovitz, and J. R. Greer, Microstructure versus flaw: Mechanisms of failure and strength in nanostructures, Nano Lett. **13**, 5703 (2013).
[14] Y. Wei, Y. Li, L. Zhu, Y. Liu, X. Lei, G. Wang, Y. Wu, Z. Mi, J. Liu, H. Wang, and H. Gao, Evading the strength-ductility trade-off dilemma in steel through gradient hierarchical nanotwins, Nature Comm. **5**, 3580 (2014).

[15] F. Sansoz, K. Lu, T. Zhu, and A. Misra, Strengthening and plasticity in nanotwinned metals, MRS Bull. **41**, 292 (2016).

[16] D. Chen and Y. Kulkarni, Entropic interactions between fluctuating twin boundaries, J. Mech. Phys. Solids **84**, 59 (2015).

[17] H. Zhang, M. I. Mendelev, and D. J. Srolovitz, Computer simulation of the elastically driven migration of a flat grain boundary, Acta Mater. **52**, 2569 (2004).

[18] M. Upmanyu, D. J. Srolovitz, L. S. Shvindlerman, and G. Gottstein, Misorientation dependence of intrinsic grain boundary mobility: Simulation and experiment, Acta Mater. **47**, 3901 (1999).

[19] H. Zhang, M. Upmanyu, and D. J. Srolovitz, Curvature driven grain boundary migration in aluminum: molecular dynamics simulations, Acta Mater. **53**, 79 (2005).

[20] K. G. F. Janssens, D. Olmsted, and E. A. Holm, Computing the mobility of grain boundaries, Nature Mater. **5**, 124 (2006).

[21] Y. Yang and S. Li, A modified synthetic driving force method for molecular dynamics simulation of grain boundary migration, Acta Mater. **100**, 107 (2015).

[22] S. M. Foiles and J. J. Hoyt, Computation of grain boundary stiffness and mobility from boundary fluctuations, Acta Mater. **54**, 3351 (2006).

[23] Z. T. Trautt, M. Upmanyu, and A. Karma, Interface mobility from interface random walk, Science **314**, 632 (2006).

[24] J. J. Hoyt, Z. T. Trautt, and M. Upmanyu, Fluctuations in molecular dynamics simulations, Math. Comput. Simul. **80**, 1382 (2010).

[25] C. Deng and C. A. Schuh, Atomistic Simulation of Slow Grain Boundary Motion, Phys. Rev. Lett. **106**, 045503 (2011).

[26] C. Deng and C. A. Schuh, Diffusive to ballistic transition in grain boundary motion studied by atomistic simulations, Phys. Rev. B **84**, 214102 (2011).

[27] M. I. Mendelev, C. Deng, C. A. Schuh, and D. J. Srolovitz, Comparison of molecular dynamics simulation methods for the study of grain boundary migration, Model. Simul. Mater. Sci. Eng. **21**, 045017 (2013).

[28] D. Chen and Y. Kulkarni, Thermal fluctuations as a computational microscope for studying crystalline interfaces: A mechanistic perspective, J. Appl. Mech. **84**, 121001 (2017).

[29] D. Chen, T. Ghoneim, and Y. Kulkarni, Effect of pinning particles on grain boundary motion from interface random walk, Appl. Phys. Lett. **111**, 161606 (2017).

[30] M. S. Green, Markoff random processes and the statistical mechanics of time-dependent phenomena. II. Irreversible processes in fluids, J. Chem. Phys. **22**, 398 (1954).

[31] R. Kubo, Statistical-mechanical theory of irreversible processes. I. General theory and simple applications to magnetic and conduction problems, J. Phys. Soc. Jpn. **12**, 570 (1957).

[32] J. P. Sethna, *Statistical Mechanics: Entropy, Order Parameters, and Complexity* (Oxford University Press, Oxford, 2006).

[33] R. K. Pathria and P. D. Beale, *Statistical Mechanics* (Elsevier, Amsterdam, 2011).

[34] J. J. Hoyt, M. Asta, and A. Karma, Method for Computing the Anisotropy of the Solid-Liquid Interfacial Free Energy, Phys. Rev. Lett. **86**, 5530 (2001).

[35] A. Stukowski, Visualization and analysis of atomistic simulation data with OVITO the open visualization tool, Model. Simul. Mater. Sci. Eng. **18**, 015012 (2010).

[36] S. J. Plimpton, Fast parallel algorithms for short-range molecular dynamics, J. Comp. Phys. **117**, 1 (1995).

[37] G. J. Ackland, G. T. Tichy, V. V. Vitek, and M. W. Finnis, Simple *n*-body potentials for the noble-metals and nickel, Phil. Mag. A **56**, 735 (1987).

[38] D. Chen and Y. Kulkarni, Elucidating the kinetics of twin boundaries from thermal fluctuations, MRS. Commun. **3**, 241 (2013).

[39] M. I. Baskes, X. W. Sha, J. E. Angelo, and N. R. Moody, Trapping of hydrogen to lattice-defects in nickel, Model. Simul. Mater. Sci. Eng. **5**, 651 (1997).

[40] Y. Mishin, M. J. Mehl, D. A. Papaconstantopoulos, A. F. Voter, and J. D. Kress, Structural stability and lattice defects in copper: Ab initio, tight-binding, and embedded-atom calculations, Phys. Rev. B **63**, 224106 (2001).

[41] H. Zhang, D. J. Srolovitz, J. F. Douglas, and J. A. Warren, Grain boundaries exhibit the dynamics of glass-forming liquids, Proc. Natl. Acad. Sci. **106**, 7735 (2009).

[42] B. Schonfelder, P. Keblinski, D. Wolf, and S. R. Phillpot, On the relationship between grain-boundary migration and grain-boundary diffusion by molecular-dynamics simulation, Mater. Sci. Forum **294-296**, 9 (1999).